8π-periodic Josephson effect in time-reversal invariant interacting Rashba nanowires

Chris J. Pedder,[1] Tobias Meng,[2] Rakesh P. Tiwari,[3] and Thomas L. Schmidt[1,*]

[1]*Physics and Materials Science Research Unit, University of Luxembourg, L-1511 Luxembourg*
[2]*Institut für Theoretische Physik, Technische Universität Dresden, 01062 Dresden, Germany*
[3]*Department of Physics, University of Basel, Klingelbergstrasse 82, CH-4056 Basel, Switzerland*

(Dated: August 3, 2015)

We investigate narrow quantum wires with strong Rashba spin-orbit coupling and electron-electron interactions. We show that virtual transitions between subbands lead to umklapp scattering which can open a partial gap in the spectrum even in the presence of time-reversal symmetry. Using the superconducting proximity effect to gap out the remaining modes, we show that the system can host zero-energy states at its edges, which are protected by time-reversal symmetry. We present the parameter regime in which these bound states will emerge. Similarly to Majorana bound states, they will produce a zero-bias peak in the differential conductance. In contrast to the Majorana fermions, however, their fourfold degeneracy leads to an 8π periodicity of the Josephson current due to tunneling of fractionalized excitations with charge $e/2$.

PACS numbers: 71.70.Ej, 73.21.Hb, 75.70.Tj, 74.50.+r.

Introduction. Systems with Rashba spin-orbit coupling (RSOC) have been of wide theoretical and experimental investigation over the last three decades, and have led to rapid growth in the areas of spintronics, spin-orbitronics [1–4], and topological phases of matter [5–7]. In particular, it was proposed that one-dimensional Rashba wires can host localized Majorana bound states when the proximity effect of a superconductor and a magnetic field perpendicular to the axis of the RSOC open spectral gaps at the Fermi energy [8–10]. In these setups, time-reversal symmetry is broken by the applied magnetic field and the twofold ground-state degeneracy is topologically protected. On the experimental side, semiconductor nanowires with strong RSOC have recently shown zero-bias conductance peaks that are thought to result from Majorana bound states [11–14].

Proposals to use non-Abelian braiding for topologically protected quantum computation [15, 16] have led to wide searches for Majorana fermions and related exotic states in experimental systems. In general, zero-energy states with non-Abelian exchange statistics are found at the boundaries between regions with trivial and non-trivial topological character. Noninteracting or weakly interacting one-dimensional helical or quasihelical states can only give rise to localized, doubly degenerate zero-energy Majorana fermions [8–10, 15, 17–22]. On the other hand, systems with strong electron-electron interactions have the potential to result in more highly-degenerate bound states, including $\mathbb{Z}_{2n}$ parafermions and non-Abelian anyons [23–30]. Most methods to engineer these states rely on explicit breaking of TR-symmetry by, e.g., magnetic fields, although proposals to realize them through spontaneous breaking of TR-symmetry exist [31–33].

In this paper, we exploit spin-umklapp scattering, whereby two spin-up fermions are scattered into two spin-down fermions, to realize fourfold degenerate zero-energy modes [32, 33] in strongly interacting one-dimensional Rashba wires. We will argue that in a finite-width quantum wire, virtual transitions to higher bands generate umklapp scattering, and that for a suitable choice of the chemical potential it will open a partial gap in a finite-length wire. Gapping out the remaining modes using proximity-induced superconductivity leads to the emergence of fourfold degenerate zero-energy bound states at the ends of the wire. Importantly, these states are symmetry-protected by time-reversal invariance. We propose that they manifest themselves in an 8π periodicity of the Josephson current.

A similar effect has recently been found for strongly interacting helical edge states of two-dimensional topological insulators [32, 33]. Experimentally, our proposed system is more amenable to investigation compared to those superconductor/topological insulator heterostructures. On the one hand, it is easier to achieve strong RSOC in, e.g., InAs or InSb quantum wires. On the other hand, it has already been shown experimentally that electron-electron interactions in these wires can be strong [34].

The outline of this paper is as follows. We introduce the model for an interacting Rashba wire system and describe the effect of inter-band virtual transitions coming from the confinement in the transversal direction. We then bosonize this model, and present renormalization group (RG) equations describing the flow of the system parameters as we change the cutoff. We find there exist regimes in which fourfold degenerate edge states can be found, and describe their implications for the Josephson effect, and the existence of fractionalized $e/2$ charges. Finally, we discuss the relevance of our work for experimental investigations.

Model. We model a finite-width wire by using the 2D Hamiltonian for a system subject to RSOC with strength α_R [2]

$$H = \frac{p_x^2 + p_y^2}{2m} + \frac{1}{2}m\omega^2 y^2 + \alpha_R(\sigma_z p_x - \sigma_y p_y), \qquad (1)$$

where $\sigma_{y,z}$ are Pauli matrices and the transversal confinement is modelled as a harmonic potential with frequency ω. The system has translational invariance along the x-direction but

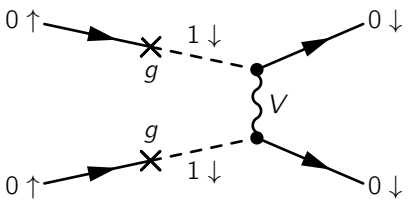

FIG. 1: A process in which virtual transitions between the lowest and the first excited subbands of the quantum wire allow for a spin-non-conserving umklapp process to be generated from a spin conserving interaction V.

is strongly confined along the y-direction. Introducing raising and lowering operators, $a^\dagger$ and a, one finds that $H = H_0 + H_1$, where

$$H_0 = \omega\left(a^\dagger a + \frac{1}{2}\right) + \frac{p_x^2}{2m} + \alpha_R \sigma_z p_x, \tag{2}$$

$$H_1 = -ig\sigma_y(a^\dagger - a), \tag{3}$$

and $g = \alpha_R\sqrt{m\omega/2}$. The form of H_1 makes it clear that transitions between neighboring subbands are always associated with a spin flip. We want to account for the possibility of virtual transitions between the lowest subband and the first excited subband with energy ω. To this purpose, we integrate out the coupling H_1 between the subbands by means of a Schrieffer-Wolff transformation, $H' = e^{-S}He^S$ where $[S, H_0] = H_1$. Up to second order in g, one finds $H' = H_0 - \frac{1}{2}[S, H_1] = p_x^2/2m + \alpha_R\sigma_z p_x$, which tells us that it would be consistent to simply ignore the dynamics in confinement direction in Eq. (1).

This trivial result changes in the interacting case where the interaction term gets modified by the Schrieffer-Wolff transformation. A generic density-density interaction potential $V(\mathbf{r}_1 - \mathbf{r}_2)$ where $\mathbf{r}_i = (x_i, y_i)$, clearly conserves spin. However, since virtual transitions to higher bands come with a spin-flip and the interaction potential $V(\mathbf{r})$ mixes states in different subbands, it can generate umklapp terms as shown in Fig. 1. After the Schrieffer-Wolff transformation, the interaction potential for the lowest subband takes the form $V' = e^{-S}Ve^S = V_\rho + V_{\rm sf} + V_{\rm sx}$, with a density-density interaction V_ρ, a spin-flip term $V_{\rm sf}$ which changes the total spin of the interacting particles (see Fig. 1), and a spin-exchange term $V_{\rm sx}$, which allows particles in the lowest band to exchange their spins, but conserves the total spin.

Placing the chemical potential at the Dirac point as shown in Fig. 2a, gives four low-energy modes at the momenta $k = 0, \pm k_F$, where $k_F = 2m\alpha_R$. Correspondingly, for small energies, we can split the field operators up into these four modes,

$$\psi_\uparrow(x) \approx e^{-ik_F x}\psi_{L\uparrow}(x) + \psi_{R\uparrow}(x), \tag{4}$$

$$\psi_\downarrow(x) \approx \psi_{L\downarrow}(x) + e^{ik_F x}\psi_{R\downarrow}(x). \tag{5}$$

Next, we express $\psi_{\alpha\sigma}(x)$ in terms of its Fourier components, $\psi_{\alpha\sigma}(x) = L^{-1/2}\sum_k e^{ikx}\psi_{\alpha\sigma,k}$, where the indices $\alpha \in \{L, R\}$, $\sigma = \uparrow, \downarrow$, and L is the length of the wire. In terms of these operators, the interaction Hamiltonians after projection to the lowest subband can be written as follows. The density-density interaction term reads

$$V_\rho = \frac{\tilde{V}(0)}{L}\sum_{\alpha,\sigma}\int dx\, \rho_{\alpha\sigma}(x)\rho_{\alpha\sigma}(x), \tag{6}$$

where the fermionic densities are defined as usual as $\rho_{\alpha\sigma}(x) = \psi^\dagger_{\alpha\sigma}(x)\psi_{\alpha\sigma}(x)$ and $\tilde{V}(q)$ is the Fourier transform of the interaction potential $V(\mathbf{r})$ projected to the lowest subband.

Due to momentum conservation, the spin-flip terms only mix terms near $k = 0$,

$$V_{\rm sf} = v_{\rm sf}\int dx\left[\psi^\dagger_{R\uparrow}(\partial_x\psi^\dagger_{R\uparrow})(\partial_x\psi_{L\downarrow})\psi_{L\downarrow} + \text{h.c.}\right], \tag{7}$$

where we retained only the leading local part $v_{\rm sf} = -2\tilde{U}(0)$ of the full interaction potential $\tilde{U}(q) = m\alpha_R^4\sum_n \Gamma_n(q)/\omega^3$. Here, $\Gamma_n(q)$ is an integral over Hermite polynomials and the interaction potential $\tilde{V}(q)$. The Hamiltonian $V_{\rm sf}$ allows for spin-umklapp scattering as shown in Fig. 2b.

Finally, most of the spin-exchange terms in $V_{\rm sx}$ can be expressed as density-density interactions, leading merely to changes in the coefficients of the terms in Eq. (6). We separate out the single non-density-density term

$$V_{\rm S} = v_{\rm S}\int dx\left(\psi^\dagger_{L\downarrow}\psi^\dagger_{R\uparrow}\psi_{L\uparrow}\psi_{R\downarrow} + \text{h.c.}\right). \tag{8}$$

$V_{\rm S}$ corresponds to an interaction between inner and outer bands with strength $v_{\rm S} = 2k_F^2\tilde{U}(k_F)$, which in the strong coupling limit results in a spin-density wave state at $q = 2k_F$. Such an interaction term has been discussed in detail in Ref. [2] and is depicted in Fig. 2c.

Bosonization. To further analyze the interacting system, we write the Hamiltonian in terms of bosonic operators $\phi_\pm$ and $\theta_\pm$ by defining

$$\psi_{R\uparrow} = \frac{U_{R\uparrow}}{\sqrt{2\pi a}}e^{-i(\phi_+ - \theta_+)}, \qquad \psi_{R\downarrow} = \frac{U_{R\downarrow}}{\sqrt{2\pi a}}e^{-i(\phi_- - \theta_-)},$$
$$\psi_{L\uparrow} = \frac{U_{L\uparrow}}{\sqrt{2\pi a}}e^{i(\phi_- + \theta_-)}, \qquad \psi_{L\downarrow} = \frac{U_{L\downarrow}}{\sqrt{2\pi a}}e^{i(\phi_+ + \theta_+)}, \tag{9}$$

where $U_{\alpha\sigma}$ are Klein factors and a denotes the short-distance cutoff. Here, $\phi_+(x)$ and $\theta_+(x)$ are canonically conjugate bosonic operators for degrees of freedom near $k = \pm k_F$, whereas $\phi_-(x)$ and $\theta_-(x)$ describe modes near $k = 0$. In these variables, the Hamiltonian consists of two Luttinger Hamiltonians for the + and − species, with approximately identical Luttinger parameters $K_\pm$, and interaction terms reflecting Eqs. (7) and (8). Moreover, one obtains terms which couple the species $\kappa_\phi\partial_x\phi_+\partial_x\phi_-$ and $\kappa_\theta\partial_x\theta_+\partial_x\theta_-$ (see Supplementary Material).

Following Ref. [2], we can diagonalize the quadratic parts of the Hamiltonian by going to the basis $\phi_{\rho,\sigma} = (\phi_+ \pm \phi_-)/\sqrt{2}$ and $\theta_{\rho,\sigma} = (\theta_+ \pm \theta_-)/\sqrt{2}$ so that

$$H_0 = \sum_{a=\rho,\sigma}\frac{v_a}{2\pi}\int dx\left[\frac{(\partial_x\phi_a)^2}{K_a} + K_a(\partial_x\theta_a)^2\right], \tag{10}$$

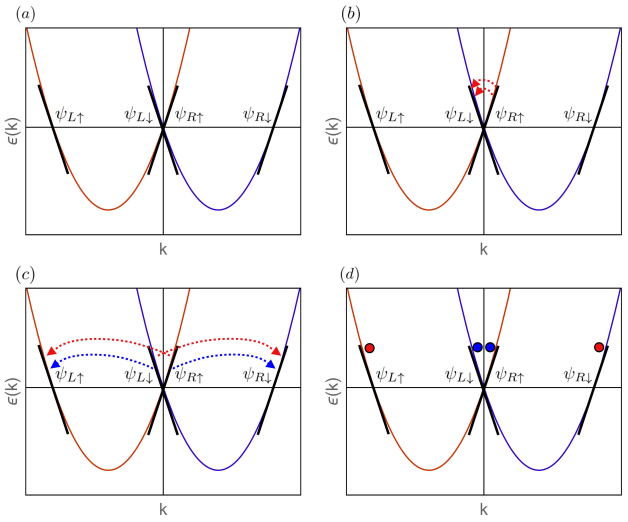

FIG. 2: (color online) Panel (a) shows the position of the chemical potential and the four low-energy linearized modes used to bosonize the system. In the other panels, we show the possible interaction processes between these modes, (b) shows umklapp scattering between the two modes near $k = 0$, (c) the "spin density wave" term that couples the modes near to $k = 0$ to those near to $k = \pm k_F$, and (d) proximity-induced s-wave superconductivity, which pairs modes of opposite physical spin.

where $v_{\rho,\sigma}$ are the respective sound velocities of the modes. For repulsive interactions, we have $K_\rho < 1$ and $K_\sigma < 1$ [2]. In addition to H_0, we obtain two competing interaction terms,

$$V_{\rm S} = \frac{g_{\rm S}}{(2\pi a)^2} \int dx\, \cos[2\sqrt{2}\theta_\sigma], \tag{11}$$

$$V_{\rm sf} = \frac{g_{\rm U}}{(2\pi a)^2} \int dx\, \cos[2\sqrt{2}(\phi_\rho - \phi_\sigma)]. \tag{12}$$

Finally, we include proximity-induced s-wave superconductivity which reads in bosonized form,

$$V_{\rm SC} = \frac{g_{\rm SC}}{(2\pi a)^2} \int dx \Big(\cos[\sqrt{2}(\theta_\rho + \theta_\sigma)] + \{\theta_\sigma \to -\theta_\sigma\}\Big). \tag{13}$$

For weak interactions, all parameters of the model can be determined in the bosonization procedure (see Supplementary Material). For strong interactions, it is more convenient to regard the parameters $v_{\rho,\sigma}$ and $K_{\rho,\sigma}$ as well as the three coupling strengths $g_{\rm S}$, $g_{\rm U}$ and $g_{\rm SC}$ as effective parameters, which may flow independently under renormalization as we change the cut-off a.

Renormalization group (RG) analysis. We calculate the flow of the various coupling constants using real-space RG calculation based on operator product expansions [36]. We find the following first-order RG equations for the coupling constants of the cosine terms,

$$\frac{dg_{\rm S}}{d\ell} = \left(2 - \frac{2}{K_\sigma}\right) g_{\rm S}, \tag{14}$$

$$\frac{dg_{\rm U}}{d\ell} = 2(1 - K_\sigma - K_\rho) g_{\rm U}, \tag{15}$$

$$\frac{dg_{\rm SC}}{d\ell} = \left(2 - \frac{1}{2K_\sigma} - \frac{1}{2K_\rho}\right) g_{\rm SC}, \tag{16}$$

implying that the spin-density wave term is always irrelevant for repulsive interactions ($K_\sigma < 1$) [2]. The umklapp term, in contrast, can become relevant for strong interactions where $K_\rho + K_\sigma < 1$. Finally, the superconducting term is relevant for $K_\rho^{-1} + K_\sigma^{-1} < 4$.

We would like to point out that for $\alpha_R = 0$, the system becomes SU(2) invariant. In that case, the umklapp term vanishes because spin is conserved and one finds the well-known Kosterlitz-Thouless RG flow which brings $K_\sigma \to 1$ as $g_{\rm S} \to 0$. In contrast, for $\alpha_R \neq 0$ K_σ is not constrained and strong repulsive interactions lead to $K_\sigma \ll 1$.

We can only continue the RG flow from the initial value $a = a_0$ all the way to $a \to \infty$ in the limit of an infinite wire at $T = 0$. For wires with length L, we stop the flow at a finite value $a_\infty < L$ as soon as one of the dimensionless coupling constants $g_{\rm SC,U}$ approaches one. The bare value of $g_{\rm SC}(a_0)$ is determined by the strength of the proximity coupling to the superconductor, which can be experimentally optimized. The bare value $g_{\rm U}(a_0)$ depends on the separation between the lowest and the first excited subband, and so depends on the transverse confinement of the wire.

To allow for the possibility of zero-energy bound states, umklapp scattering needs to gap out the modes near $k = 0$, whereas proximity-induced superconductivity should open a gap for the modes at $k = \pm k_F$. Since superconductivity affects in principle all modes, this is only possible if at the end of the RG flow $|g_{\rm U}(a_\infty)| > |g_{\rm SC}(a_\infty)| > 0$. Strong electron-electron interactions result in $K_\rho < 1/2$ and $K_\sigma < 1/2$, which a priori makes the umklapp term relevant and the superconducting term irrelevant. However, since the RG flow stops at a finite length scale, $|g_{\rm SC}(a_\infty)| > 0$ is nevertheless possible.

To demonstrate the existence of localized zero-energy bound states, we use the unfolding transformation described in Refs. [29, 37]. It can be used to map our system with length L and open boundary conditions to a system of length $2L$ and periodic boundary conditions. In this transformation, the (ϕ_+, θ_+) degrees of freedom, which are gapped out by superconductivity, are mapped on the range $\tilde{x} \in [0, L]$. The (ϕ_-, θ_-) degrees of freedom, which are gapped out by umklapp scattering, are mapped on the range $\tilde{x} \in [L, 2L]$. The unfolded system is identical to the helical edge state considered in Refs. [32, 33]. It was shown there that this system hosts fourfold degenerate zero-energy interface states at $\tilde{x} = L$ and $\tilde{x} = 2L$. Undoing the unfolding transformation, these interface states turn into bound states at the end of the wire. These bound states can be described as $\mathbb{Z}_4$ parafermions, lead to a fourfold degenerate ground state, and carry fractional charge $e/2$ [32, 33].

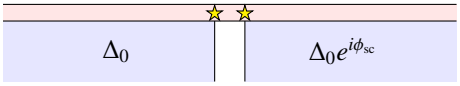

FIG. 3: Experimental setup for the measurement of the 8π periodic Josephson effect. Two superconductors underneath a Rashba wire are held at a phase difference ϕ_{sc}. Fractionally charged bound states are indicated by stars.

Josephson effect. A zero-bias conductance peak is a possible experimental signature of localized Majorana fermions. However, such peaks could arise from other mechanisms, e.g., disorder [38, 39], and do not directly indicate the degeneracy of the states involved. In particular, the fourfold degenerate bound state we propose would lead to the same zero-bias anomaly in transport measurements, albeit at vanishing magnetic field. To uniquely discriminate these bound states, we instead propose to discover the presence of bound states via the periodicity of the Josephson effect, similarly to the corresponding proposal for Majorana fermions [19, 40].

To investigate the effect of the zero-energy bound states on the Josephson effect, we follow the logic of Ref. [32, 33] and consider an arrangement with two superconducting contacts with phase difference ϕ_{sc} placed on top of a Rashba wire partially gapped by umklapp scattering, see Fig. 3 which is analogous to the experimental setup in Ref. [40]. The parts of the wire underneath the edges of the superconductors will host zero-energy modes with charge $e/2$, which will dominate the transport at low energies. Tunnelling of a single quasiparticle through the junction changes the parity of the end states. In order to satisfy the boundary conditions due to the applied superconducting phase, *four* $e/2$ quasiparticles must tunnel via the bound states, leading to an 8π periodic Josephson effect [32]. The time-reversal breaking of the superconducting phase difference causes a slight lifting of the fourfold degeneracy, but for realistic parameters this shift is negligible [32].

Several works [41, 42] suggest that in a spinless, one-dimensional system, the greatest achievable toplogical degeneracy is twofold, leading to the statement that only Majorana fermions can exist in one-dimensional systems. Our system does not contradict this theorem because in our case the ground state degeneracy is not entirely topological. Indeed, it can be viewed as a twofold topological degeneracy combined with a twofold degeneracy due to time-reversal symmetry [10]. The second can be lifted by local perturbations such as a magnetic field. In that case, only the topological part of the ground state degeneracy survives, and one recovers a 4π periodicity of the Josephson effect associated with Majorana bound states [19].

Discussion. We have predicted an 8π periodicity of the Josephson current in strongly interacting quantum wires with RSOC coupled to an s-wave superconductor, heralding the emergence of fractionalized excitations with charge $e/2$. It is important to note that these modes do not have topological protection, but are protected by time-reversal symmetry.

Note that the opening of the umklapp gap at $k = 0$ is independent of the proximity-induced superconductivity, and will occur rather generically. In a wire with sufficiently strong RSOC and electron-electron interactions this gap would lead to a reduction of the conductance of from $2e^2/h$ to e^2/h as the chemical potential approaches the Dirac point. A similar phenomenon has recently been observed in GaAs wires [43] and our results may provide another interpretation for this experiment if RSOC is sufficiently strong in the GaAs nanowires used. In interacting InSb or InAs wires [34], where RSOC is typically stronger, a measurement of the conductance as a function of the chemical potential could demonstrate the proposed effect conclusively. Finally, umklapp scattering has just recently been invoked to explain the observed conductance reduction in InAs/GaSb topological insulator edge states [44]. Introducing a weak superconducting proximity effect in either of these types of wires or edge states will then lead to the creation of bound states and allow the observation of the 8π periodic Josephson effect.

It may be possible to realize similar bound states in 1D chains of alkali atoms in cold atomic gas experiments, where RSOC can be engineered [45], and where one has direct control over the interaction strength via the confinement induced resonance [46, 47]. Tuning this resonance to give repulsive interactions near $k = 0$ and attractive interactions near $|k| = k_F$ would provide the competition between umklapp scattering and pairing required to generate bound states.

Acknowledgements. We would like to thank Meera Parish, Stephan Rachel, Peter Schmitteckert, Björn Trauzettel, and Alexander Zyuzin for helpful discussions. TLS & CJP are supported by the National Research Fund, Luxembourg under grant ATTRACT 7556175. TM is funded by Deutsche Forschungsgemeinschaft through GRK 1621 and SFB 1143. RPT acknowledges financial support from the Swiss National Science Foundation.

* Electronic address: thomas.schmidt@uni.lu

[1] J. Sinova, D. Culcer, Q. Niu, N. A. Sinitsyn, T. Jungwirth, and A. H. MacDonald, Phys. Rev. Lett. **92**, 126603 (2004).
[2] S. Gangadharaiah, J. Sun, and O. A. Starykh, Phys. Rev. B **78**, 054436 (2008).
[3] D. Awschalom and N. Samarth, Physics **2**, 50 (2009).
[4] I. M. Miron, G. Gaudin, S. Auffret, B. Rodmacq, A. Schuhl, S. Pizzini, J. Vogel, and P. Gambardella, Nat. Mat. **9**, 230 (2010).
[5] S. Nakosai, Y. Tanaka, and N. Nagaosa, Phys. Rev. Lett. **108**, 147003 (2012).
[6] T. Das and A. V. Balatsky, Nat. Comm. **4** (2013).
[7] P. King, R. C. Hatch, M. Bianchi, R. Ovsyannikov, C. Lupulescu, G. Landolt, B. Slomski, J. Dil, D. Guan, J. Mi, et al., Phys. Rev. Lett. **107**, 096802 (2011).
[8] Y. Oreg, G. Refael, and F. von Oppen, Phys. Rev. Lett. **105**, 177002 (2010).
[9] R. M. Lutchyn, J. D. Sau, and S. Das Sarma, Phys. Rev. Lett. **105**, 077001 (2010).
[10] E. Sela, A. Altland, and A. Rosch, Phys. Rev. B **84**, 085114 (2011).

[11] M. T. Deng, C. L. Yu, G. Y. Huang, M. Larsson, P. Caroff, and H. Q. Xu, Nano Letters **12**, 6414 (2012).
[12] V. Mourik, K. Zuo, S. M. Frolov, S. R. Plissard, E. P. A. M. Bakkers, and L. P. Kouwenhoven, Science **336**, 1003 (2012).
[13] I. van Weperen, S. R. Plissard, E. P. A. M. Bakkers, S. M. Frolov, and L. P. Kouwenhoven, Nano Letters **13**, 387 (2013).
[14] S. Nadj-Perge, I. K. Drozdov, J. Li, H. Chen, S. Jeon, J. Seo, A. H. MacDonald, B. A. Bernevig, and A. Yazdani, Science **346**, 602 (2014).
[15] A. Y. Kitaev, Physics-Uspekhi **44**, 131 (2001).
[16] C. Nayak, S. H. Simon, A. Stern, M. Freedman, and S. Das Sarma, Rev. Mod. Phys. **80**, 1083 (2008).
[17] D. A. Ivanov, Phys. Rev. Lett. **86**, 268 (2001).
[18] L. Fu and C. L. Kane, Phys. Rev. Lett. **100**, 096407 (2008).
[19] L. Fu and C. L. Kane, Phys. Rev. B **79**, 161408 (2009).
[20] M. Sato and S. Fujimoto, Phys. Rev. B **79**, 094504 (2009).
[21] M. Sato, Y. Takahashi, and S. Fujimoto, Phys. Rev. Lett. **103**, 020401 (2009).
[22] J. Alicea, Rep. Prog. Phys. **75**, 076501 (2012).
[23] G. Moore and N. Read, Nucl. Phys. B **360**, 362 (1991), ISSN 0550-3213.
[24] M. Cheng, Phys. Rev. B **86**, 195126 (2012).
[25] M. Barkeshli and X.-L. Qi, Phys. Rev. X **2**, 031013 (2012).
[26] N. H. Lindner, E. Berg, G. Refael, and A. Stern, Phys. Rev. X **2**, 041002 (2012).
[27] M. Barkeshli, C.-M. Jian, and X.-L. Qi, Phys. Rev. B **87**, 045130 (2013).
[28] D. J. Clarke, J. Alicea, and K. Shtengel, Nat. Comm. **4**, 1348 (2013).
[29] Y. Oreg, E. Sela, and A. Stern, Phys. Rev. B **89**, 115402 (2014).
[30] N. Kainaris and S. T. Carr, Phys. Rev. B **92**, 035139 (2015).
[31] J. Klinovaja and D. Loss, Phys. Rev. B **90**, 045118 (2014).
[32] F. Zhang and C. L. Kane, Phys. Rev. Lett. **113**, 036401 (2014).
[33] C. P. Orth, R. P. Tiwari, T. Meng, and T. L. Schmidt, Phys. Rev. B **91**, 081406(R) (2015).
[34] R. Hevroni, V. Shelukhin, M. Karpovski, M. Goldstein, E. Sela, H. Shtrikman, and A. Palevski, arXiv:1504.03463 (2015).
[35] See Supplemental Material for further details of the bosonization proceedure and the renormalization group analysis.
[36] J. Cardy, *Scaling and Renormalization in Statistical Physics* (Cambridge University Press, 1996).
[37] T. Giamarchi, *Quantum physics in one dimension* (2004).
[38] D. I. Pikulin, J. P. Dahlhaus, M. Wimmer, H. Schomerus, and C. W. J. Beenakker, New J. Phys. **14**, 125011 (2012).
[39] J. Liu, A. C. Potter, K. T. Law, and P. A. Lee, Phys. Rev. Lett. **109**, 267002 (2012).
[40] L. P. Rokhinson, X. Liu, and J. K. Furdyna, Nat. Phys. **8**, 795 (2012).
[41] L. Fidkowski and A. Kitaev, Phys. Rev. B **83**, 075103 (2011).
[42] A. M. Turner, F. Pollmann, and E. Berg, Phys. Rev. B **83**, 075102 (2011).
[43] C. P. Scheller, T.-M. Liu, G. Barak, A. Yacoby, L. N. Pfeiffer, K. W. West, and D. M. Zumbühl, Phys. Rev. Lett. **112**, 066801 (2014).
[44] T. Li, P. Wang, H. Fu, L. Du, K. A. Schreiber, X. Mu, X. Liu, G. Sullivan, G. A. Csathy, X. Lin, et al., arXiv:1507.08362 (2015).
[45] V. Galitski and I. B. Spielman, Nature (2013).
[46] I. Bloch, J. Dalibard, and W. Zwerger, Rev. Mod. Phys. **80**, 885 (2008).
[47] T. Bergeman, M. G. Moore, and M. Olshanii, Phys. Rev. Lett. **91**, 163201 (2003).

SUPPLEMENTAL MATERIAL

Interactions

The most general spin-conserving interaction term is given by

$$\hat{V} = \sum_{\sigma_1\sigma_2} \int d^2r_1 d^2r_2 \psi^\dagger_{\sigma_1}(\mathbf{r}_1)\psi^\dagger_{\sigma_2}(\mathbf{r}_2)V(|\mathbf{r}_1 - \mathbf{r}_2|) \times \psi_{\sigma_2}(\mathbf{r}_2)\psi_{\sigma_1}(\mathbf{r}_1). \tag{17}$$

We transform this potential Eq.(17) using the Schrieffer-Wolff transformation, and then project onto the lowest subband. The Hamiltonian in momentum space in this sector is

$$\hat{H} = \hat{H}_\mathrm{k} + \hat{V}_\rho + \hat{V}_\mathrm{sf} + \hat{V}_\mathrm{sx}, \tag{18}$$

where the kinetic energy takes the form

$$\hat{H}_\mathrm{k} = \sum_{\sigma,p} \left(\frac{p^2}{2m} + \alpha_\mathrm{R}\sigma p \right) \psi^\dagger_{p,\sigma}\psi_{p,\sigma}, \tag{19}$$

and the operators $\psi^\dagger_{p,\sigma}$ and $\psi_{p,\sigma}$ create and annihilate an electron of spin σ and momentum p. The potential terms are then $\hat{V}_\rho$, the density-density interaction

$$\hat{V}_\rho = \frac{1}{L_y} \sum_{\sigma_1\sigma_2} \sum_{p,p',q} \tilde{V}(q) \psi^\dagger_{p+q,\sigma_1}\psi^\dagger_{p'-q,\sigma_2}\psi_{p',\sigma_2}\psi_{p,\sigma_1}, \tag{20}$$

and then the spin flip and spin exchange terms

$$\hat{V}_\mathrm{sf} = \frac{1}{L_y} \sum_{\sigma} \sum_{p,p',q} \tilde{U}(q)(2p' - q)(2p + q) \times \psi^\dagger_{p+q,\sigma}\psi^\dagger_{p'-q,\sigma}\psi_{p',-\sigma}\psi_{p,-\sigma}, \tag{21}$$

$$\hat{V}_\mathrm{sx} = \frac{1}{L_y} \sum_{\sigma} \sum_{p,p',q} \tilde{U}(q)(2p' - q)(2p + q) \times \psi^\dagger_{p+q,\sigma}\psi^\dagger_{p'-q,-\sigma}\psi_{p',\sigma}\psi_{p,-\sigma}, \tag{22}$$

where $\tilde{V}(q)$ and $\tilde{U}(q)$ are defined in the main body of the paper. We now project these terms onto the low energy states of the system and retain only terms allowed by momentum conservation, giving

$$\hat{V}_\rho = \frac{\tilde{V}(0)}{L_y} \sum_{\alpha,\sigma} \int dx\, \rho_{\alpha,\sigma}(x)\rho_{\alpha,\sigma}(x). \tag{23}$$

The fermionic densities are $\rho_{\alpha\sigma}(x) = \psi^\dagger_{\alpha\sigma}(x)\psi_{\alpha\sigma}(x)$. In order to conserve momentum, the spin flip terms may only mix terms near $q = 0$, so $\hat{V}_\mathrm{sf}$ reads

$$\hat{V}_{\rm sf} = -2\tilde{U}(0)\int dx\left(\psi^\dagger_{R\uparrow}(\partial_x\psi^\dagger_{R\uparrow})(\partial_x\psi_{L\downarrow})\psi_{L\downarrow} + \text{h.c.}\right) \quad (24)$$

Finally, the spin exchange terms only lead to a small change in terms already present in $\hat{V}_\rho$, so we can account for them by a change of the interaction parameters, but we should keep separate the one term which may not be written as a density-density interaction;

$$\hat{V}_{\rm S} = 2k_F^2\tilde{U}(k_F)\int dx\Big(\psi^\dagger_{L\downarrow}\psi^\dagger_{R\uparrow}\psi_{L\uparrow}\psi_{R\downarrow} + \psi^\dagger_{R\downarrow}\psi^\dagger_{L\uparrow}\psi_{R\uparrow}\psi_{L\downarrow}\Big). \quad (25)$$

We now bosonize these terms. Using the standard identity that $\rho_{\alpha,\sigma} = \partial_x\phi_{\alpha,\sigma}/2\pi$, we find that at weak coupling, the complete interaction Hamiltonian $\hat{V} = \hat{V}_\rho + \hat{V}_{\rm sf} + \hat{V}_{\rm sx}$ becomes

$$\begin{aligned}\hat{V} = &\frac{1}{(2\pi)^2}\int dx\Big([\tilde{V}(0)+4\tilde{U}(0)]((\partial_x\phi_+)^2+(\partial_x\phi_-)^2) \\ &+\tilde{V}(0)((\partial_x\theta_+)^2+(\partial_x\theta_-)^2)\Big) \\ &+\frac{1}{(2\pi)^2}\int dx\Big([8\tilde{U}(0)-2k_F^2\tilde{U}(k_F)]\partial_x\phi_+\partial_x\phi_- \\ &+2k_F^2\tilde{U}(k_F)\partial_x\theta_+\partial_x\theta_-\Big) \\ &+\frac{1}{(2\pi a)^2}\int dx\, 2k_F^2\tilde{U}(k_F)e^{i(2\theta_+-2\theta_-)}\end{aligned} \quad (26)$$

We note at this point that the Luttinger parameters for the two species are equal in the weak coupling limit. The coupling between the species given by the terms $\kappa_\phi\partial_x\phi_+\partial_x\phi_-$ where $\kappa_\phi = 8\tilde{U}(0)-2k_F^2\tilde{U}(k_F)$ and $\kappa_\theta\partial_x\theta_+\partial_x\theta_-$ where $\kappa_\theta = 2k_F^2\tilde{U}(k_F)$. These can be removed by going to the charge-spin basis described in the text, which yields Eqn.(9), with new Luttinger parameters

$$\begin{aligned}K_\rho &= \frac{K+\gamma_\theta/2}{1/K+\gamma_\phi/2}, \\ K_\sigma &= \frac{K-\gamma_\theta/2}{1/K-\gamma_\phi/2},\end{aligned} \quad (27)$$

and renormalised Fermi velocities $v_\rho = v_F K_\rho$ and $v_\sigma = v_F K_\sigma$. $v_F = \alpha_{\rm R}$ is the Fermi velocity for the non-interacting modes. Note that these expressions are only valid at weak coupling. However, the division into a pair of non-interacting Luttinger Hamiltonians with three competing cosine interaction terms forms our prototypical model for the strongly interacting case we consider.

Renormalization Group

We calculate the scaling dimensions of the operators above, and also the second order RG flow for the parameters K_ρ and K_σ. We diagonalize the non-interacting Hamiltonian Eq.(10) by introducing the fields $\varphi_{\alpha a} = \alpha\sqrt{K_a}\phi_a - \theta_a/\sqrt{K_a}$, where $a = \rho,\sigma$, and as before $\alpha = R, L$, which gives

$$\begin{aligned}H_0 = &\frac{v_\rho}{(2\pi a)^2}\int dx\left((\partial_x\varphi_{\rho R})^2+(\partial_x\varphi_{\rho L})^2\right) \\ &+\frac{v_\sigma}{(2\pi a)^2}\int dx\left((\partial_x\varphi_{\sigma R})^2+(\partial_x\varphi_{\sigma L})^2\right).\end{aligned} \quad (28)$$

The scaling dimensions of the operators are calculated by normal-ordering them with respect to the creation and annihilation operators of the diagonal Hamiltonian (28). We find

$$V_{\rm S} = \frac{g_{\rm S}}{(2\pi a)^2}\left(\frac{L}{2\pi a}\right)^{-2/K_\sigma}\int :\cos[2\sqrt{2}\theta_\sigma]: . \quad (29)$$

Asserting that this term cannot change as a result of the RG step $a \to a - da = a(1+d\ell)$ and $g_{\rm S} \to g_{\rm S} + dg_{\rm S}$ gives the first-order RG equation for $g_{\rm S}$ as

$$\frac{dg_{\rm S}}{d\ell} = \left[2 - \frac{2}{K_\sigma}\right]g_{\rm S}. \quad (30)$$

Under normal ordering, the umklapp term becomes

$$\begin{aligned}V_{\rm U} = &\frac{g_{\rm U}}{(2\pi a)^2}\left(\frac{L}{2\pi a}\right)^{-2(K_\rho+K_\sigma)} \\ &\times\int dx :\cos[2\sqrt{2}(\phi_\rho-\phi_\sigma)]:,\end{aligned} \quad (31)$$

and so has the first-order RG equation

$$\frac{dg_{\rm U}}{d\ell} = \left[2(1-K_\sigma-K_\rho)\right]g_{\rm U}. \quad (32)$$

The superconducting term has scaling behaviour

$$\begin{aligned}V_{\rm SC} = &\frac{g_{\rm SC}}{(2\pi a)^2}\left(\frac{L}{2\pi a}\right)^{-\frac{1}{2K_\rho}-\frac{1}{2K_\sigma}} \\ \times\int dx\Big(&:\cos[\sqrt{2}(\theta_\rho+\theta_\sigma]: + :\cos[\sqrt{2}(\theta_\rho-\theta_\sigma]:\Big).\end{aligned} \quad (33)$$

giving an RG equation

$$\frac{dg_{\rm SC}}{d\ell} = \left[2 - \frac{1}{2K_\sigma} - \frac{1}{2K_\rho}\right]g_{\rm SC}. \quad (34)$$

Continuing to second order in the spin density wave term, we find the real time partition function takes the form

$$Z_2 = -\frac{g_S^2}{8(2\pi a)^4}\left(\frac{L}{2\pi a}\right)^{-4/K_\sigma}\int dx_1\, dx_2\, dt_1\, dt_2 \times :\cos[2\sqrt{2}\theta_\sigma(x_1,t_1)]::\cos[2\sqrt{2}\theta_\sigma(x_2,t_2)]:. \quad (35)$$

We then normal order the two individually normal ordered cosines, and keep only the part which gives us a new scaling compared to the first-order term to get

$$Z_2 = -\frac{g_S^2 a^{4/K_\sigma}}{8(2\pi a)^4}\int dx_1\, dx_2\, dt_1\, dt_2\, [m_\sigma^+ m_\sigma^-]^{-2/K_\sigma} \times :\cos[2\sqrt{2}\theta_\sigma(x_1,t_1)]\cos[2\sqrt{2}\theta_\sigma(x_2,t_2)]:, \quad (36)$$

where we have defined $m_\sigma^\pm = a - iv_\sigma(t_2 - t_1) \pm i(x_2 - x_1)$. Because they are now under normal ordering, we can expand the cosines for small $x_2 - x_1$, to get

$$Z_2 = -\frac{g_S^2 a^{4/K_\sigma}}{(2\pi a)^4}\int dx_1\, dx_2\, dt_1\, dt_2\, [m_\sigma^+ m_\sigma^-]^{-2/K_\sigma} \times (x_2 - x_1)^2 : (\partial_x\theta_\sigma)^2 :. \quad (37)$$

This is a renormalization of the coefficient of $(\partial_x\theta_\sigma)^2$, that is to say a renormalization of K_σ.

We now re-express this as a term in the first-order partition function of the operator $(\partial_x\theta_\sigma)^2$; we therefore shift to centre of mass $\tilde{x} = x_1 + x_2$ and relative $x = x_2 - x_1$ coordinates (same for t), and leave the integration over the centre of mass coordinates alone. In order to calculate the coefficient of the term $(\partial_x\theta_\sigma)^2$, we do the RG step $a \to a - da = a(1 + d\ell)$ inside the integral only, which gives us an integral form for the coefficient κ_1

$$\kappa_1 = \int_{-\infty}^{\infty} dx \int_{-\infty}^{0} dt \frac{x^2((1 - iv_\sigma t)^2 + x^2)^{-2/K_\sigma}}{(2\pi)^4 v_\sigma} \quad (38)$$

which turns up in the renormalization of K_σ, $dK_\sigma = \kappa_1 g_S^2 d\ell$. We can compute this integral exactly, to get

$$\kappa_1 = \frac{1}{(2\pi)^4 v_\sigma}\frac{\sqrt{\pi}\Gamma[2/K_\sigma - 3/2]}{2\Gamma[2/K_\sigma]}. \quad (39)$$

This term has a weak, linear dependence on K_σ, so only allowing for small changes of K_σ we may treat it as approximately constant.

Similar calculations for the terms in g_U and g_{SC} give us the coupled RG equations below

$$\frac{dK_\sigma}{d\ell} = \kappa_1 g_S^2 - \kappa_2 g_U^2 K_\sigma^2 + \kappa_3 g_{SC}^2, \quad (40)$$

$$\frac{dK_\rho}{d\ell} = -\kappa_2 g_U^2 K_\rho^2 + \kappa_3 g_{SC}^2. \quad (41)$$

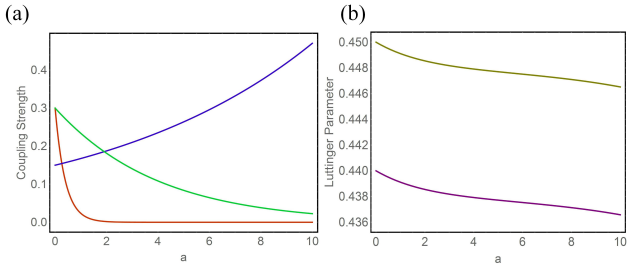

FIG. 4: (color online) This figure shows the RG flow for the full, coupled, second order RG equations given in this section. The initial values are $g_S = g_{SC} = 0.3$, $g_U = 0.15$ and $K_\rho = K_\sigma = 0.45$. Panel (a) shows the RG flow of couplings g_S (red), g_{SC} (green) and g_U (blue) as the cutoff a changes, panel (b) shows the flow of K_ρ (yellow) and K_σ (pink). When the blue curve crosses the green curve in the figures, the ground state becomes fourfold degenerate.

κ_2 is given by the integral

$$\kappa_2 = \frac{4a^{4(K_\rho+K_\sigma)+1}}{(2\pi a)^4}\int_{-\infty}^{0} dt \int_{-\infty}^{\infty} dx\, x^2 \times \partial_a\left\{[(a - iv_\rho t)^2 + x^2]^{-2K_\rho}[(a - iv_\sigma t)^2 + x^2]^{-2K_\sigma}\right\}, \quad (42)$$

and κ_3 by

$$\kappa_3 = \frac{2a^{\left(\frac{1}{K_\rho}+\frac{1}{K_\sigma}\right)+1}}{(2\pi a)^4}\int_{-\infty}^{0} dt \int_{-\infty}^{\infty} dx\, x^2 \times \partial_a\left\{[(a - iv_\rho t)^2 + x^2]^{-\frac{1}{2K_\rho}}[(a - iv_\sigma t)^2 + x^2]^{-\frac{1}{2K_\sigma}}\right\}. \quad (43)$$

Note that the use of the full, second order RG equations does not change qualitatively the result given in the main text using only the first order RG equations, as the second order terms only result in small changes in K_ρ and K_σ.